Available online at www.sciencedirect.com

ScienceDirect

Procedia Engineering 102 (2015) 590 – 601

Procedia Engineering

www.elsevier.com/locate/procedia

The 7th World Congress on Particle Technology (WCPT7)

Studies on the preparation, characterization and intracellular kinetics of JD27-loaded human serum albumin nanoparticles

Shujuan Yan[a],Hongling Zhang[a],Junyan Piao[a],Yan Chen[a],Shulin Gao[a],Chunyun Lu[a],Lifeng Niu[a],Yadan Xia[a],Yang Hu[a],Ruibin Ji[a],Haigang Wang[a],Xia Xu[a]*

[a]*School of Pharmaceutical Sciences, Zhengzhou University,100 Kexue Avenue, Zhengzhou 450001 , PR China;*

Abstract

JD27 is a derivatives of active ingredient extracted from Rabdosia which includes a functional group of 1,2,3-Triazoles. It is considered as a promising anti-cancer drug candidate because of its low toxicity and broad-spectrum anti-cancer activity. However, the clinical application of JD27 has been limited by its poor solubility. Albumin is an attractive macromolecular carrier, which has been widely used in nanoparticle preparation. Compared with other drug delivery systems, drug-loaded albumin nanoparticles showed a series of advantages such as solubilization of hydrophobic drug, biodegradable, biocompatible and so on. In this study, JD27-loaded human serum albumin nanoparticles (JD27-NPs) were obtained using an established desolvation method and they were characterized by particle size, zeta potential, encapsulation efficiency, surface morphology and in vitro drug release studies. In addition, their cytotoxic activities, intracellular kinetics and cell membranes permeability were evaluated in EC-9706 cells. The experiment results showed that the particle size, zeta potential, and encapsulation efficiency were (276.5±8.26) nm, (−41.4±7.21) mV and 82.2%±5.09%, respectively. SEM images suggest that JD27–NPs were a round shape, similar uniform size and smooth surface. Drug release studies indicated JD27-NPs had the properties of sustained release. The results of cytotoxic activities suggest that antitumor efficacy of JD27–NPs is higher than JD27 in EC-9706 cells. According to the results of intracellular kinetics, the concentration of JD27-NPs in the cell could reach the peak concentration after 2 hour and gradually decreases with time lasted. The AUC0-12h and MRT of JD27-NPs are significantly higher than that in JD27 ($P<0.05$). JD27-NPs have advantages to keep a higher and steadier intracellular concentration than JD27 which shows JD27-NPs have priority in application. The results of Hoechst 33258 staining suggested that the permeability of the cells membrane can be changed with the different concentration and treatment time of JD27. In conclusion, albumin nanopaticles may act as a useful and safe carrier for JD27.JD27-NPs will be a promising formulation for cancer therapy in future.

Selection and peer-review under responsibility of Chinese Society of Particuology, Institute of Process Engineering, Chinese Academy of Sciences (CAS)

* Xia Xu. Tel.: +86-0371-6665-9519; fax: +86-0371-6665-9519.
E-mail address: xuxia@zzu.edu.cn

Selection and peer-review under responsibility of Chinese Society of Particuology, Institute of Process Engineering, Chinese Academy of Sciences (CAS)
doi:10.1016/j.proeng.2015.01.133

Keywords: JD27; albumin nanoparticles; cytotoxicity ; Hoechst 33258 ; intracellular kinetics

1. Introduction

1,2,3-Triazole which is a reactive group can be found in a wide range of bioactive molecules such as antimicrobial[1,2], anti-hypersensitivity[3], anti-tuberculosis [4,5],anti-inflammatory agents[6] and anti-HIV agents [7,8].In recent years, much attention has been paid to their anticancer activity, recent research report that1,2,3-Triazoles exhibit effective anticancer activity [9-16]. JD27 which includes a functional group of 1,2,3-Triazoles is a derivatives of active ingredient extracted from Chinese traditional medicine Rabdosia rubescens. JD27 is considered as a promising anti-cancer drug candidate because of its low toxicity and broad-spectrum anti-cancer activity. However, JD27 shows a very low water solubility, which limits its clinical use. Large efforts are ongoing to develop drug carrier systems that improve drug solubility.

Among the different formulation strategies used to deliver insoluble drugs, albumin-based nanoparticle is a very effective approach to improve drug solubility. Albumin, a multifunctional protein carrier for drug delivery, has drawn considerable attention in the pharmaceutical fields in view of non-toxic, non-immunogenic, good biocompatible and biodegradable [17-19].Albumin nanoparticles have gaining increasing interesting due to a higher capacity of loading hydrophilic drugs. Different from nanoparticles made of synthetic polymers, HSA nanoparticles are considered no significant side effects and well-tolerated in vivo [20-22], which is supported by the findings of several clinical studies on HSA-based particle products such as Albunex™[23,24] and Abraxane™[25,26]. Furthermore, it has a unique feature of entering tumor cells through the well-known gp60 pathway which can enhance the bioavailability and distribution of drug, reducing the body's response towards drug resistance and diminishing their toxicity [27, 28].Therefore, nanoparticles made of HSA will be a promising strategy for targeted delivery of anticancer drugs to tumor cells.

Albumin nanoparticles can be prepared by several methods including desolvation [29, 30], emulsification [31, 32], self-assembly [33, 34], nab-technology [35, 36] techniques. Among all the methods, desolvation process is a robust and reproducible method for the denaturation of albumin [37]. Zhao et al [29] successfully prepared nanoparticles of folate-conjugated water insoluble paclitaxel-loaded bovine serum albumin by a desolvation technique. The paclitaxel-loaded bovine serum albumin can significantly increased water solubility of paclitaxel. Li et al[30] produced oridonin loaded bovine serum albumin nanoparticle (ORI-BSA-NP) and oridonin loaded galactosylated bovine serum albumin nanoparticle (ORI-GB-NP) by the desolvation technique The results of characteristics and in vitro drug release of ORI-GB-NP show that the nanoparticles possessed fine physicochemical characteristics and will be a stable delivery system for poorly soluble oridonin.

The objective of study is to develop a novel nano-drug delivery system JD27-loaded human serum albumin nanoparticle (JD27-NPs). Firstly, JD27-NPs were obtained using an established desolvation method [38]. Then, the physicochemical characteristics including particle size, zeta potential, encapsulation efficiency and surface morphology and in vitro drug release studies were determined. In addition, cytotoxic activities and intracellular kinetics of these nanoparticles were also investigated.

2. Materials and methods

2.1. Chemicals and reagents

Human serum albumin (HSA, purity 99%, 65,000Da) obtained from Sigma (Steinheim, Germany). JD27 was a gift of School of Pharmaceutical Sciences of Zhengzhou University School. Hoechst 33258 fluorescence apoptosis detection kit was purchased by Keygen Biotechnology Development Co., Ltd.. RPMI 1640 cell culture medium and 3-(4,5-dimethylthiazol-2-yl)-2,5-diphenyltetrazolium bromide(MTT) were bought from Gibco Invitrogen. Ethanol and ethyl acetate were used as analytic reagents. Methanol and acetonitrile were of high performance liquid chromatography grade. An EC-9706 human esophageal cancer cell line was obtained from the Chinese Academy of Sciences Cell Bank.

2.2. Preparation of JD27-NPs

JD27-NPs were prepared using an established desolvation method [38]: an amount of HSA was dissolved in distilled water and the pH was adjusted to 9 with 0.1 M NaOH. A certain amount of JD27 was dissolved in 10ml ethanol. The solution was continuously (1ml/min) added to albumin solution under permanent stirring (600 rpm) at room temperature. Following the desolvation process the particles were cross-linked by adding predetermined volume of 25% glutaraldehyde (10-40μl) and stirred at room temperature for 12h. In order to remove unreacted chemicals and free HSA molecules, the resulting nanoparticles were purified by three cycles of differential centrifugation (15,000rpm, 30 min) and finally redispersion in water.

2.3. Measurement of particle size and zeta potential

Size distribution and zeta potential of JD27-NPs were measured by dynamic light scattering DLS (Zetasizer Nano ZS-90, Malvern, UK). The samples were diluted 1:50 with purified water and were measured at a temperature of 25°C.Every sample was measured for three times.

2.4. Determination of encapsulation efficiency

JD27-NPs were separated from the aqueous suspension medium by ultracentrifugation of 15,000rpm at 4°C for 30min.The amount of free JD27 in the clear supernatant was determined by high performance liquid chromatography(HPLC, 1100 Agilent, USA).The HPLC system comprised of a pump and UV-Vis detector with a Diamonsil ^{TM} ODS C18 column(4.6mm×150mm，5μm) was used for the quantification of JD27 in the samples. The mobile phase was a mixed of water and acetonitrile (70:30) containing 0.1% phosphoric acid . The flow rate was set to 1ml/min with detection at 240nm. Aliquot of 20μl clear supernatant was injected into HPLC. The working curve was obtained by standard JD27 solutions with different concentrations over the range of 0.25-100.0 μg/ml.

Encapsulation efficiency was calculated using the following equations:

$$\text{Encapsulation efficiency} = \frac{W_{total} - W_{free}}{W_{total}} \times 100\%$$

2.5. Surface morphology

The shape and surface morphology of JD27-NPs were investigated by scanning electron micrograph (SEM, JSM-5610LV, JEOL Ltd., Tokyo, Japan).

2.6. In vitro drug release studies

0.5 ml JD27-NPs (2mg/ml) solution was dialyzed (cutoff Mw14 kDa) against 25ml release PBS buffer at 37°C in a water bath at 100rpm. Sample were taken at predetermined times outside of the release medium and the same volume of fresh buffer was added, and the concentrations of JD27 were determined by HPLC under the above chromatographic conditions. The release experiments were repeated three times and the cumulative percentage of drug release was reported.

2.7. Cell culture

The EC-9706 cells were cultured in RPMI1640 medium with 10% fetal calf serum (FCS) plus penicillin (100 IU/ml) and streptomycin (100μg/ml). The EC-9706 cells were propagated in an incubator with a humidified

atmosphere of 5%CO2 in air at 37°C and seeded in new medium every 2-3 days, and were in the exponential phase of growth at the time of inclusion in assay.

2.8. In vitro cytotoxicity

MTT method is used to compare in vitro cytotoxicity between JD27-NPs and JD27 on EC-9706 cells. Briefly, EC-9706 (104 cells) were plated in each well of a 96-well plate and were allowed to adhere and spread for 24h. The cells were incubated with serial concentrations of JD27 and JD27-NPs (2-32μg/ml)at 37°C for 24h and 48h.MTT solution (20μl of 5mg/ml) was added to each well, and incubated for an additional 4h. After 4h, MTT-formazan crystals were dissolved in 150μl DMSO. The absorbance was measured on microplate reader (BIO-Rad, United States) at the wavelength 490nm and compared with control, untreated cells. For all experiments, results were obtained from triplicate experiments using SPSS software (version 17.0).

At the same time , in order to directly perceived the effect of JD27-NPs on EC-9706, the EC-9706 were treated respectively with different concentrations of JD27-NPs (4μg/ml,16μg/ml,32μg/ml) for 48h, and the cell morphology was observed with inverted microscope.

2.9. Hoechst 33258 staining

EC-9706 cells were seeded at 2×105 cells/well in 6-well plates and incubated for 24h (Place a clean sterile blood cover sheet in each well of a 6-well plate so that tumor cells can be adhere on it). Then the medium was replaced with fresh medium containing different concentrations of JD27 (16μg/ml, 32μg/ml). After incubation for different durations(4h and 8h), the culture plates in cell culture medium was discarded, the cells were fixed for 10 min at 4°C using4% formaldehyde, then formaldehyde was discarded and the cells were washed gently with PBS twice. Finally, 100μl Hoechst 33258 was added, and changes of the blue fluorescence in stained cells were observed by using an fluorescence microscopy (Nikon, Eclipse 80i).

2.10. Intracellular kinetics studies

2.10.1. HPLC condition

Concentrations of JD27 in cell lysates were detected using HPLC systems. The samples were passed through a reverse-phase column (Diamonsil TM ODS C18 column,4.6mm×150mm,5μm). The mobile phase was a mixed of water and acetonitrile (75:25) containing 0.1% phosphoric acid. The flow rate was set to 1ml/min with detection at 240nm.

2.10.2. Determination of intracellular JD27

After incubation with JD27-NPs or JD27 the medium was removed, and cells were washed three times with cold phosphate buffer saline (PBS). Cells were harvested by trypsinization prior to counting. The intracellular concentrations of JD27 were determined as follows: the cells were ruptured by ultrasonic cell crusher (JY92-Ⅱ, Ningbo Chi Bio-Technology Co., Ltd.). A volume of 6.0 ml ethyl acetate was added to the simples as extractant. The mixture was vortex-mixed for 5min and centrifuged for 15min at 4500rpm.5.5ml of the organic supernatant was transferred to another tube and evaporated at 40°C to dryness under an N2 stream. The residue was reconstituted in 100μl of mobile phase methanol and following vortex mixing for 5 min and centrifugation at 12000 rpm for 15min, 20μl of supernatant was injected into the HPLC system. Concentrations of JD27 in cell lysates were calculated relative to a calibration curve.

2.10.3. Intracellular kinetics studies

EC-9706 cells were seeded in culture dish and incubated for 24h. The medium was then removed, and fresh medium containing same concentrations of JD27 and JD27-NPs (8μg/ml) was added. After incubation for different durations (0.5h, 1h, 2h, 4h, 8h,12h). The concentrations of intracellular were determined as described above. The results were obtained from triplicate experiments using Kinetica software (Version 4.4.1).

3. Results and discussion

3.1. Characterization of nanoparticles

JD27-NPs were characterized for size, zeta potential, encapsulation efficiency and Surface morphology. The size and zeta potential were (276.5±8.26) nm (Fig.1b) and (−41.4±7.21) mV (Fig.1c), respectively. In Fig 2，JD27-NPs were observed by SEM, which had a round shape, smooth surface and similar uniform size. The obtained JD27-NPs were well dispersed without aggregation (Fig.1a).

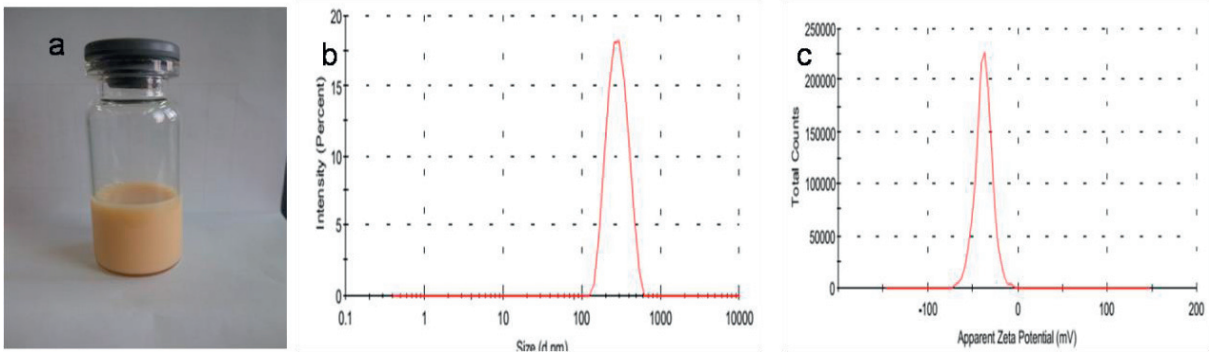

Fig.1 Characterization of JD27-NPs (a) JD27-NPs; (b) Particle size of JD27-NPs;(c) zeta potential of JD27-NPs.

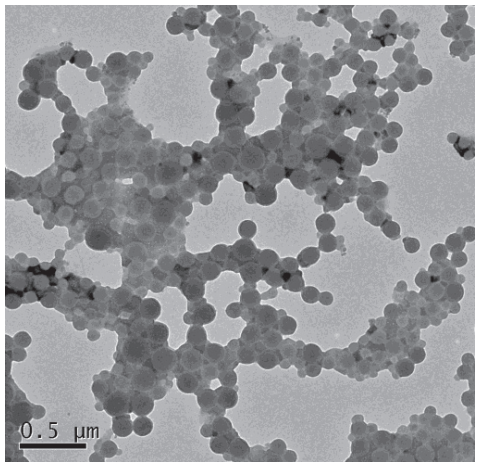

Fig.2 Scanning electron micrograph (SEM) of JD27-NPs

In desolvation process, single factor design including the concentration of HSA and JD27, the amount desolvating agent and cross-linker, cross-linking time and pH were investigated to optimize the formula and technology for preparing JD27-NPs. According to the single factor test, the amount of desolvating agent added and the pH of HSA solution were identified as the major factor determining the particle size. Varying these parameters, mean particle diameters could be adjusted to about 270nm, higher pH values leading to smaller nanoparticles. Taking the size, the zeta potential, especially the entrapment efficiency into account, we identified the best formula for preparing JD27-NPs.

Fig.3a illustrates the in vitro release of JD27solution and JD27-NPs.The accumulative release of JD27-NPs was about 15% at 0.5 h, and 60% at 48 h, respectively .Meanwhile, the accumulative release of JD27 solution was about 40% at 0.5 h and 93% at 48 h, respectively. The release rate of JD27-NPs significantly slower than that in pure JD27 solution, and it became slower with increasing time. The above data indicated that JD27-NPs were showing the sustained-release effect. The calibration curve of JD27 was y =9727.6x + 609.08 with a correlation coefficient of 0.9999 in the concentration range of 0.25-100.0 μg/ml. (y: peak area; x: concentration of JD27, μg/ml) (Fig.3b). According to the calibration curve, the encapsulation efficiency was 82.2%±5.09%.

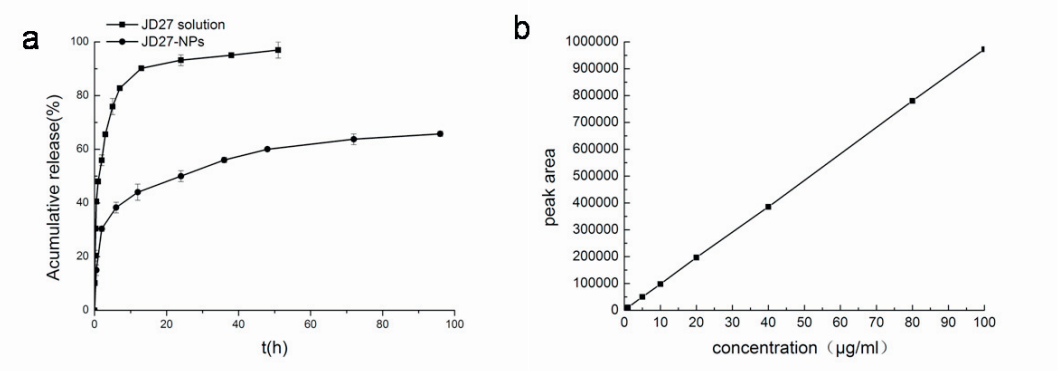

Fig. 3 (a) Release profiles of JD27 from JD27-NPs and JD27 solution (mean ± SD, n=3); (b) Calibration curve of JD27.

The study of drug release indicated JD27-NPs had sustained release effect which enabled JD27 release more stably and continuously. Sustained release effect of JD27-NPs provides the possibility to fight continually against cancer cells, resulting in decreased cancer cell viability. The generally sustained and controlled release profile of JD27-NPs facilitated the application of nanoparticles for the delivery of anticancer drugs.

3.2. In vitro cytotoxicity

The cytotoxicity studies of JD27-NPs and JD27 on EC-9706 cells were carried out with different concentrations of JD27-NPs and JD27. In this text, we designed the blank NPs group as the contrast to reduce its influences on results .As shown in Fig.4, cell inhibitions of blank NPs remained below 10% at all concentrations. These data indicates that the blank NPs had no obvious toxic effect on EC-9706 cells. According to the Fig.4, as the increasing of concentration and time of exposure of JD27-NPs and JD27, the effect against the EC-9706 cells gradually increased. Inhibition efficiency of JD27-NPs on EC-9706 cells was higher than JD27 ($P < 0.05$) at all the time point .In the table1,the IC50 of JD27 and JD27-NPs at 24h were 31.925μg/ml and 27.483μg/ml while the IC50 of JD27 and JD27-NPs were obtained at a concentration of 27.873μg/ml and 10.611μg/ml at 48h.Regarding the IC50 values, JD27-NPs exhibited a higher inhibition efficiency on EC-9706 cells than JD27($P < 0.05$) at 24h and 48h. Fig.5 illustrates the morphology of EC-9706 cells exposed to JD27-NPs by inverted microscope after 48h. We found that some cells is round and float , the contact of cells becomes loose, the proliferation was slowed down and the particle increased in cytoplasm with the increase of drug concentration and treatment time.

Table1 IC50 Values of JD27 and JD27-NPs on EC-9706 cells (mean ± SD, n=3)

Incubation	IC50(μg/ml)	
Time(h)	24h	48h
JD27	31.925±1.35	27.873±0.73
JD27-NPs	27.483±2.67	10.611±1.56

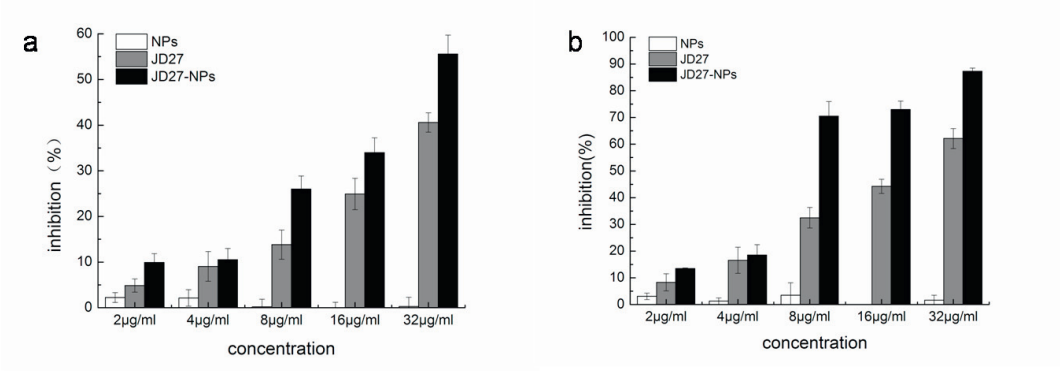

Fig .4 Inhibition of JD27 and JD27-NPs on EC-9706 cells at different time (a) 24h (mean ± SD, n=3); (b) 48h (mean ± SD, n=3)

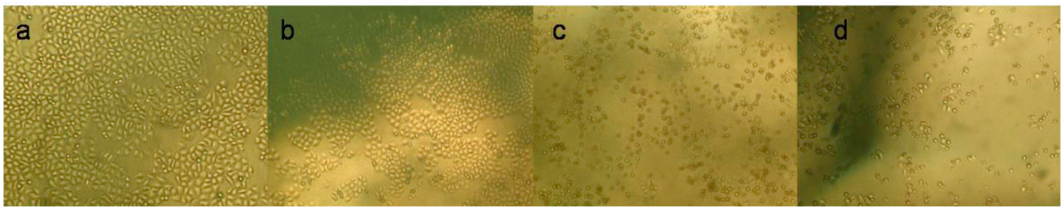

Fig.5 Morphology of EC-9706 cells exposed to JD27-NPs by inverted microscope after 48h (200×) (a)Control;(b)4μg/ml; (c)16.0 μg/ml;(d)32μg/ml

JD27-NPs significantly inhibits the growth of EC-9706 cell line by time-dependent and concentration-dependent in 24h and 48h, suggesting that the delivery system could efficiently cross cell membranes and afford higher antitumor efficacy on EC-9706 cells. JD27-NPs will be a promising formulation for cancer therapy in future.

3.3. Hoechst 33258 staining

Blue-fluorescent Hoechst 33258 may pass through the integral membrane of live cells. Condensed chromatin of apoptotic cells stained with Hoechst 33258 can emit more brightly blue-fluorescent than the looser chromatin of normal cells, which can monitor changes of nuclear associated with apoptosis. Therefore, the level of Hoechst 33258 uptake indicates the permeability change of the cells membrane.

Influence of JD27 on cell nuclear morphology of EC-9706 cells was presented in Fig.6 after 8h and 12h of incubation with different concentrations of JD27. Apoptotic cells staining with Hoechst 33258 can emit bright blue fluorescence. As shown in the Fig.6, percentage of apoptotic cells significant increased in a concentration-dependent and time-dependent manner, indicating that the level of Hoechst 33258 uptake increased. The enhanced uptake of Hoechst 33258 indicated that JD27 could change the permeability of cell membrane. With the increase of cell membrane permeability, the more JD27 could efficiently cross cell membranes resulting in a better anti-tumor effect.

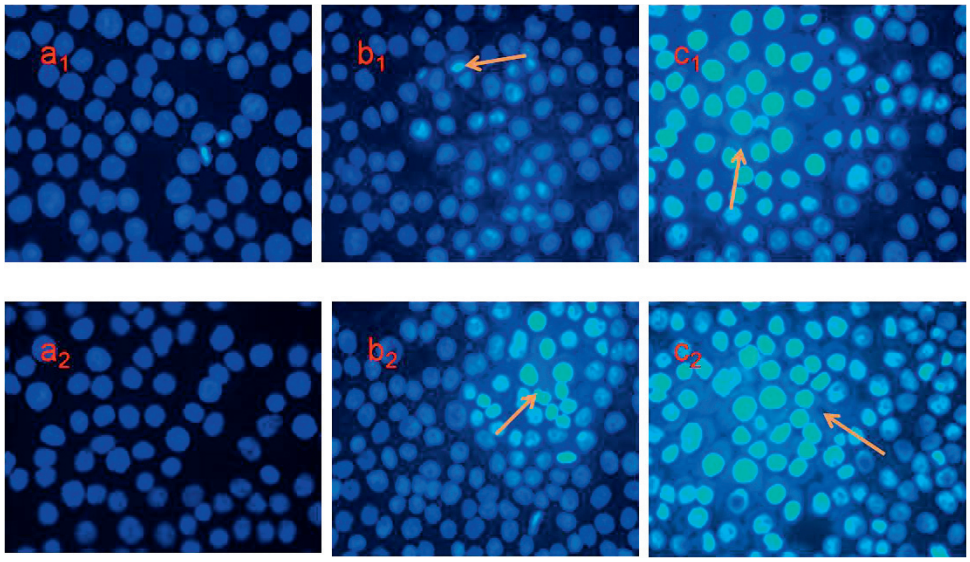

Fig.6 Influence of JD27 on cell nuclear morphology of EC-9706 cells with Hoechst 33258 staining（400×）($a_1$and a_2) control; (b_1)cells treated with 16μg/ml for 4h; (c_1)cells treated with 16μg/ml for 8h; (b_2) cells treated with 32μg/ml for 4h; (c_2) cells treated with 32μg/ml for 8h.

3.4. Intracellular kinetics studies

The Intracellular kinetics curve of JD27 and JD27-NPs are shown in (Fig.7a). Uptake of JD27 and JD27-NPs increased as the time went on, reaching to the highest amount after 2h. As shown in the Table2 in comparison with JD27, $AUC_{0\text{-}12h}$, MRT ,$t_{1/2}$ Kel, $t_{1/2}$ Ka of JD27-NPs were higher than JD27.The calibration curve of intracellular kinetics was y=0.008x-0.2178 with a correlation coefficient of 0.9967 in the concentration range of 25.0-800.0 ng/ml. (y: peak area; x: concentration of JD27 in cell lysates , ng/ml) (Fig.7b).

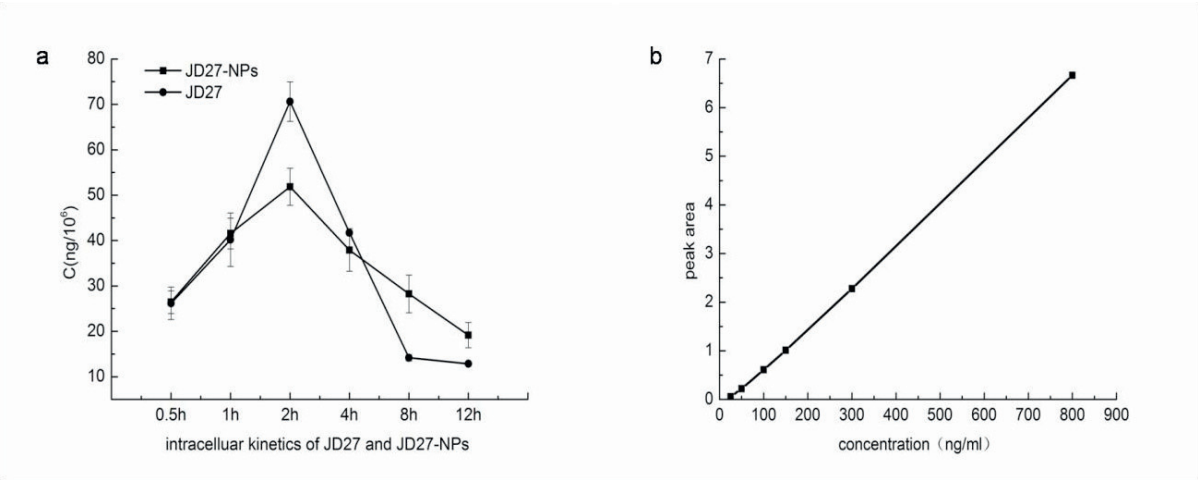

Fig. 7 (a)Intracellular kinetics of JD27andJD27-NPs in EC-9706 cells.EC-9706 cells were treated with 8μg/ml of JD27or JD27-NPs at 0.5,1,2,4,8 and12h time points (mean ± SD, n=3); (b) Calibration curve of intracellular kinetics

Table 2 Kinetics parameters of JD27 and JD27-NPs after uptake by EC-9706 cells (mean ± SD, n=3)

Formulation	Parameters	Unit	Value
JD27	kel	1/h	0.192429±0.02
	t1/2 Ka	h	0.170375±0.06
	MRT	h	4.41248±0.26
	Cmax	ng/10^6 cells	60.6693±0.31
	Tmax	h	1.57148±0.16
	t1/2 Kel	h	3.60209±0.23
	AUC	(ng/10^6 cells)·h	366.85±4.95
JD27-NPs	kel	1/h	0.2940859±0.08
	t1/2 Ka	h	0.191012±0.05
	MRT	h	9.84517±3.79
	Cmax	ng/10^6 cells	50.9572±10.22
	Tmax	h	1.41722±0.04
	t1/2 Kel	h	7.36717±2.46
	AUC	(ng/10^6 cells)·h	574.883±11.08

The results of intracellular kinetics were consistent with previously obtained drug release curves in vitro, indicating that the JD27-NPs had a delayed-release effect. Compared with JD27, the JD27-NPs had obtained a much higher $AUC_{0\text{-}12h}$ ($P<0.05$), which indicating JD27-NPs can enhance the drug bioavailability on EC-9706 cells. Meanwhile, JD27-NPs also obtained a much longer MRT ($P<0.05$), which stood for prolonged drug duration on EC-9706 cells. Intracellular parameters showed that JD27-NPs have advantages to keep a higher and steadier intracellular concentration than JD27, which shows JD27-NPs can promote JD27 intracellular uptake of EC-9706 cells. It also indicates that JD27-NPs could make JD27 release more stably and continuously. JD27-NPs are likely to have a significant potential for in vivo anti-tumor efficacy in future.

4. Discussion

In the area of pharmaceutical research, nanoparticulate delivery systems are gradually became a hot spot research because nanocarriers have a series of advantages such as improve drug solubility, protect drugs from degradation, increase penetration and intracellular distribution . Nanoparticles based on albumin have received considerable interest due to high binding capacity of hydrophobic drugs and biocompatibility without any serious side effects. The smaller size (50-300 nm) and controlled release properties can improve patient compliance and acceptance. Moreover, human serum albumin (HSA) was selected as an ideal candidate for drug delivery due to its readily available, biodegradable and priority uptake. Thus, HSA is the ideal material to make nanoparticles for drug delivery [39-41]. Albumin-bound (NAB-) paclitaxel ABI-007(trade name Abraxane®; the company Abraxis BioScience and AstraZeneca), a novel , albumin-bound , 130-nm particle formulation of paclitaxel is one of the sucessful strategies to solve solvent-related problems of paclitaxel[42]. Recently, the U.S. Food and Drug Administration have approved it for pretreated metastatic breast cancer patients. In this paper, we successfully prepared JD27-NPs with a particle size of about 270nm and high encapsulation efficiency. SEM images showed that JD27-NPs was a round shape, smooth surface and similar uniform size, which making the JD27-NPs have a higher penetration into tumor cells with an increased antitumor activity, compared with JD27. In addition, Human serum albumin substitute bovine serum albumin as nanocarriers to prepare the JD27-NPs could avoid a possible immunologic response in vivo. JD27-NPs show significant advantages to JD27 and will be a high potential formulation for the treatment of cancer.

Gp60 is an endothelial cell membrane 60-kDa glycoprotein and has a high binding capacity to albumin. Albumin binding to a gp60 receptor seems to lead to combination of gp60 and an intracellular protein (caveolin-1) and

subsequently invagination of the cell membrane to form transcytotic vesicles. Thereby, the transcytosis of albumin across the endothelium of blood vessels is achieved through the well-known gp60 pathway which promoting the albumin-bound drugs into tumor cells [43-48].Furthermore, SPARC which is known as an extracellular matrix glycoprotein acid rich in cysteine is often seen in some neoplasms .It can bind to albumin, which further facilitates the intratumor accumulation of albumin-bound drugs [49-54]. In short, albumin will be actively and selectively recognized and bound by the two different proteins rich in the tumor tissues, which may explain the reason why albumin is known to accumulate in some tumors. Kim et al. prepared the CCM-loaded HSA-NPs by nab-technology and investigated the potential mechanisms about enhanced accumulation of curcumin (CCM) in tumor. They found that the endothelial transcytosis of CCM-HSA-NPs was completely suppressed by β-methyl cyclodextrin(known as a inhibitor of caveolar mediated transcytosis)[36].

In this paper, according to the results of intracellular kinetics, compared with JD27, the JD27-NPs had obtained a much higher $AUC_{0\text{-}12h}$ ($P<0.05$) and a much longer MRT ($P<0.05$), which indicating JD27-NPs can enhance the drug bioavailability and prolong drug duration in EC-9706 cells. Therefore, JD27-NPs could improve JD27 intracellular uptake of EC-9706 cells .The in situ data suggest that JD27-NPs uptake and antitumor activity was significantly increased by the use of nanoparticle delivery system. So we infer the possible mechanisms were to be due to increased transendothelial gp60-mediated transport and SPARC-albumin interaction [55-57]. In addition, the mechanisms of accumulation of JD27-NPs nanoparticles in EC-9706 remain to be identified next.

5. Conclusion

In summary, this study demonstrated that JD27, a water insoluble anticancer drug, could be successfully loading into albumin nanoparticles with a particle size of about 270nm and high encapsulation efficiency. In the view of the data of in vitro cytotoxicity obtained in this study, it can be concluded that albumin loading with JD27 had higher inhibition efficiency on EC-9706 cells than JD27. The intracellular kinetics was definitely proved that compared to JD27, JD27-NPs could enhance the drug bioavailability and prolong drug duration on EC-9706 cells. It is believed that JD27-NPs has priority in application and could be used to investigate the vivo effects of JD27.Our investigations suggest that albumin nanoparticles may act as a useful and safe carrier for JD27. JD27-NPs will be a promising formulation for cancer therapy in future. In addition, the vivo characters of JD27 remain to be identified.

References

[1] J.A. Demaray, J.E. Thuener, M.N. Dawson, et al., Synthesis of triazoleoxazolidinones via a one-pot reaction and evaluation of their antimicrobial activity, Bioorg. Med. Chem. Lett. 18 (2008) 4868-4871.

[2] X.L. Wang, K. Wan, C.H. Zhou, Synthesis of novel sulfanilamide-derived 1,2,3-triazoles and their evaluation for antibacterial and antifungal activities, Eur. J. Med. Chem. 45 (2010) 4631-4639.

[3] D.R. Buckle, D.J. Outred, C.J.M. Rockell, et al., Studies on v-triazoles. 7. Antiallergic 9-oxo-1H, 9H-benzopyrano [2,3-d]-v-triazoles, J. Med. Chem. 26 (1983) 251-254.

[4] M.S. Costa, N. Boechat, E.A. Rangel, et al., Synthesis, tuberculosis inhibitory activity, and SAR study of N-substituted -phenyl-1,2,3-triazole derivatives, Bioorg. Med. Chem. 14 (2006) 8644-8653.

[5] S.R. Patpi, L. Pulipati, P. Yogeeswari, et al., Design, Synthesis, and structure-activity correlations of novel dibenzo[b, d]furan, dibenzo[b, d]thiophene, and N-methylcarbazole clubbed 1,2,3-triazoles as potent inhibitors of mycobacterium tuberculosis, J. Med. Chem. 55 (2012) 3911-3922.

[6] R.D. Simone, M.G. Chini, I. Bruno,et al., Structure-based discovery of inhibitors of microsomal prostaglandin E2 synthase-1,5-lipoxygenase and 5-lipoxygenase-activating protein: promising hits for the development of new anti-inflammatory agents, J. Med. Chem. 54 (2011) 1565-1575.

[7] M. Whiting, J.C. Tripp, Y.C. Lin, et al., Rapid discovery and structure-activity profiling of novel inhibitors of human immunodeficiency virus type 1 protease enabled by the copper(I)-catalyzed synthesis of 1,2,3-triazoles and their further functionalization, J. Med. Chem. 4 (2006) 7697-7710.

[8] M.J. Giffin, H. Heaslet, A. Brik, et al., A copper(I)-catalyzed 1,2,3-triazole azidealkyne click compound is a potent inhibitor of a multidrug-resistant HIV-1 protease variant, J. Med. Chem. 51 (2008) 6263-6270.

[9] M.J. Fray,D.J. Bull, C.L. Carr, et al., Structure activity relationships of 1,4-dihydro-(1H,4H)-quinoxaline-2,3-dionesas N-methyl-D-aspartate (glycine site) receptor antagonists. 1. Heterocyclic substituted 5-alkyl derivatives, J. Med. Chem. 24 (2001) 1951-1962.

[10] D. Imperio, T. Pirali, U. Galli, et al., Replacement of the lactone moiety on podophyllotoxin and steganacin analogues with a 1,5-disubstituted 1,2,3-triazole via ruthenium-catalyzed click chemistry, Bioorg. Med. Chem. 15 (2007) 6748-6757.

[11] L.S. Kallander, Q. Lu, W. Chen, et al., 4-Aryl-1,2,3-triazole: a novel template for a reversible methionine aminopeptidase 2 inhibitor, optimized to inhibit angiogenesis in vivo, J. Med. Chem. 48 (2005) 5644-5647.
[12] F. Pagliai, T. Pirali, E.D. Grosso, et al., Rapid synthesis of triazole-modified resveratrol analogues via click chemistry, J. Med. Chem. 49 (2006) 467-470.
[13] L. Cafici, T. Pirali, F. Condorelli, et al., Solution-phase parallel synthesis and biological evaluation of combretatriazoles, J. Comb. Chem. 10 (2008) 732-740.
[14] C.B. Yim, I. Dijkgraaf, R. Merkx, et al., Synthesis of DOTA-conjugated multimeric [Tyr3]Octreotide peptides via a combination of Cu(I)-catalyzed "Click" cycloaddition and thio acid/sulfonyl azide "sulfo-click" amidation and their in vivo evaluation, J. Med. Chem. 53 (2010) 3944-3953.
[15] J. Yoon, J.S. Ryu, A rapid synthesis of lavendustin-mimetic small molecules by click fragment assembly, Bioorg. Med. Chem. Lett. 20 (2010) 3930-3935.
[16] J. Vantikommu, S. Palle, P.S. Reddy, et al., Synthesis and cytotoxicity evaluation of novel 1,4-disubstituted 1,2,3-triazoles via CuI catalysed 1,3-dipolar cycloaddition, Eur. J. Med. Chem. 45 (2010) 5044-5050
[17] A.B. MacAdam, Z.B. Shafi, S.L. James, et al., Preparation of hydrophobic and hydrophilic albumin microspheres and determination of surface carboxylic acid and amino residues, Int. J. Pharm. 151(1997)47–55
[18] P.R. Orapin, K. Richard, S. James, Albumin microspheres as a drug delivery system: relation among turbidity ratio, degree of cross-linking, and drug release, Pharm. Res. 10(1993) 1059–1065.
[19] M. Yun, E.B. Micheal, T. Dolores, et al., Human serum albumin nanoparticles for efficient delivery of Cu, Zn superoxide dismutase gene, Mol. Vis. 13(2007)746–757.
[20] S. Dreis, F. Rothweiler, M. Michaelis, et al., Preparation, characterisation and maintenance of drug efficacy of doxorubicin-loaded human serum albumin (HSA) nanoparticles. Int. J. Pharm. 341(2007)207-214.
[21] J.M. Irache, S. Espuelas. Albumin nanoparticles, in: C. Kumar (Ed), Biological and pharmaceutical nanomaterials, Wiley-VCH, Germany, 2006. pp. 185-208.
[22] F. Kratz, Albumin as a drug carrier: design of prodrugs, drug conjugates and nanoparticles. J. Control. Release.132 (2008) 171-183.
[23] S.B .Feinstein, J. Cheirif , F.J. Ten Cate , et al., Safety and efficacy of a new transpulmonary ultrasound contrast agent: initial multicenter clinical results, J. Am. Coll. Cardiol.16 (1990) 316-324.
[24] B. Geny, B. Mettauer, B. Muan, et al., Safety and efficacy of a new transpulmonary echo contrast agent in echocardiographic studies in patients. J. Am. Coll. Cardiol. 22(1993)1193–1198.
[25] B. Damascelli, G. Cantù, F. Mattavelli, et al., Intraarterial chemotherapy with polyoxyethylated castor oil free paclitaxel, incorporated in albumin nanoparticles (ABI-007): phase I study of patients with squamous cell carcinoma of the head and neck and anal canal: preliminary evidence of clinical activity. Cancer. 92(2001) 2592–2602.
[26] N.K. Ibrahim, N. Desai ,S. Legha , et al., Phase I and pharmacokinetic study of ABI-007, a Cremophor-free, protein-stabiliz
-ed, nanoparticle formulation of paclitaxel, Clin. Cancer Res. 8 (2002) 1038-1044.
[27]M.A. Foote, Using nanotechnology to improve the characteristics of antineoplastic drugs: improved characteristics of nab-paclitaxel compared with solvent-based paclitaxel, Biotechnol. Annu. Rev. 13(2007)345-357.
[28] C. Tiruppathi, T. Naqvi, Y. Wu, et al., Albumin mediates the transcytosis of myeloperoxidase by means of caveolae in endothelial cells. Proc. Natl. Acad .Sci .USA 101(2004)7699-7704.
[29] D. Zhao, X. Zhao, Y. Zu, et al., Preparation, characterization, and in vitro targeted delivery of folate-decorated Paclitaxel -loaded bovine serum albumin nanoparticles, Int. J. Nanomedicine 5 (2010)669–677.
[30] C. Li, D. Zhang, H. Guo, Preparation and characterization of galactosylated bovine serum albumin nanoparticles for liver-targeted delivery of oridonin, Int. J. Pharm. 448(2013)79-86.
[31] G.V. Patil, Biopolymer albumin for diagnosis and in drug delivery, Drug Dev. Res.58 (2003) 219–247.
[32] L. Yang, F. Cui, D. Cun, A. Tao, K. Shi, W. Lin, et al.Preparation, characterization and biodistribution of the lactone form of 10-hydroxycamptothecin (HCPT)-loaded bovine serum albumin (BSA) nanoparticles, Int. J. Pharm. 340 (2007) 163–172.
[33] R. Xu, M. Fisher, R.L. Juliano, et al., Targeted albumin-based nanoparticles for delivery of amphipathic drugs, Bioconjug. Chem. 22 (2011) 870–878.
[34] J. Gong, M. Huo, J. Zhou, et al, Synthesis, characterization, drug-loading capacity and safety of novel octyl modified serum albumin micelles, Int. J. Pharm. 376 (2009) 161–168.
[35] N. Desai. Nanoparticle albumin bound (nab) technology: targeting tumors through the endothelial gp60 receptor and SPARC, Nanomedicine .3 (2007) 337-346.
[36] T. H. Kim, H.H.Jiang, Y.S.Youn, et al. Preparation and characterization of water-soluble albumin-bound curcumin nanoparticles with improved antitumor activity.Int. J. Pharm. 403 (2011) 285–291.
[37] K. Langer, S. Balthasar, V. Vogel, et al., Optimization of the preparation process for human serum albumin (HSA) nanoparticles, Int. J. Pharm. 257 (2003) 169–180.
[38] C. Weber, C. Coester, J. Kreuter, et al., Desolvation process and surface characteristics of protein nanoparticles. Int. J. Pharm. 194 (2000)91–102.
[39] V.P. Torchilin, Nanotechnology in Drugs, second ed., Imperial College Press, London, 2008.
[40] S.K. Sahoo, V. Labhasetwar, Nanotech approaches to drug delivery and imaging, Drug Discov. Today 8 (2008) 1112-1120.
[41] P. Couvreur, C. Vauthier, Nanotechnology: intelligent design to treat complex disease, Pharm. Res. 23 (2006) 1417-1450.
[42] R.M.N. Kumar, Nano and microparticles as controlled drug delivery devices, J. Pharm. Pharm. Sci. 3 (2000) 234–258.

[43] U. Schilling, E.A. Friedrich, H. Sinn, et al., Design of compounds having enhanced tumour uptake, using serum albumin as a carrier: Part II. in vivo Studies. Int. J. Rad. Appl. Instrum. B. 19(1992)685-695.
[44] J.E. Schnitzer, P. Oh, Antibodies to SPARC inhibit albumin binding to SPARC, gp60, and microvascular endothelium. Am. J. Physiol.263 (1992)H 1872-1879.
[45] C. Tiruppathi, A. Finnegan, A.B. Malik, Isolation and characterization of a cell surface albumin binding protein from vascular endothelial cells. Proc. Natl. Acad. Sci. USA. 93(1996) 250-254.
[46] N.P. Desai, V. Trieu, Z. Yao, et al., Increased antitumor activity, intratumor paclitaxel concentrations, and endothelial cell transport of Cremophor-free, albumin-bound paclitaxel, ABI-007, compared with Cremophor-based paclitaxel. Clin Cancer Res 12(2006)1317-1324.
[47] S.M. Vogel, R.D. Minshall, M. Pilipovic, et al., Albumin update and transcytosis in endothelial cells in vivo induced by albumin-binding protein. Am. J. Physiol. Lung Cell Mol. Physiol. 281(2001) L1512-1522.
[48] N.P. Desai, V. Trieu, R. Yao, et al., Increased transport of nanoparticle albumin-bound paclitaxel (ABI-007) by endothelial gp60-mediated caveolar transcytosis: A pathway inhibited by Taxol. 16th Annual Meeting of the European Organisation for Research and Treatment of Cancer-National Cancer Institute–American Association for Cancer Research..Geneva, Switzerland, 2004.
[49] P.L. Porter, E.H. Sage, T.F. Lane, et al., Distribution of SPARC in normal and neoplastic human tissue. J. Histochem. Cytochem. 43(1995) 791-800.
[50] Y.W. Kim, Y.K. Park, J. Lee, et al., Expression of osteopontin and osteonectin in breast cancer. J. Korean Med. Sci. 13(1998) 652-657.
[51] R. Thomas, L.D. True, J.A. Bassuk, et al., Differential expression of osteonectin/SPARC during human prostate cancer progression. Clin. Cancer Res. 6(2000)1140-1149.
[52] V. Trieu, B. Damascelli, P. Soon-Shiong, et al. ,SPARC expression in head and neck cancer correlates with tumor response to nanoparticles albumin-bound paclitaxel (nab-paclitaxel, ABI-007, Abraxane),97th American Association of Cancer Research Annual Meeting, Washington, DC, USA, 2006.
[53] N.P. Desai, V. Trieu, R. Yao, et al. SPARC expression in breast tumors may correlate to increased tumor distribution of nanoparticle albumin-bound paclitaxel (ABI-007) vs Taxol,27th Annual San Antonio Breast Cancer Symposium, San Antonio, USA ,2004.
[54] T.J. Brown, P.A. Shaw, X. Karp, et al., Activation of SPARC expression in reactive stroma associated with human epithelial ovarian cancer. Gynecol. Oncol. 75(1999)25-33.
[55] K. Paál, J. Müller, L. Hegedûs, High affinity binding of paclitaxel to human serum albumin. Eur. J. Biochem. 268(2001)2187–2191.
[56] J. Cortes, C. Saura, Nanoparticle albumin-bound (nab™)-paclitaxel: improving efficacy and tolerability by targeted drug delivery in metastatic breast cancer, EJC Suppl. 8 (2010) 1–10.
[57] M.J. Hawkins, P. Soon-Shiong, N. Desai, Protein nanoparticles as drug carriers in clinical medicine, Adv. Drug Deliv. Rev. 60 (2008) 876–885.